XXI IMEKO World Congress "Measurement in Research and Industry"
August 30 – September 4, 2015, Prague, Czech Republic

CHARGE-TRANSFER-BASED SIGNAL INTERFACE FOR DIFFERENTIAL CAPACITIVE SENSORS

Jorge E. Gaitán-Pitre, Ramon Pallas-Areny

Universitat Politècnica de Catalunya, BarcelonaTech (UPC), Castelldefels, Spain, ramon.pallas@upc.edu

Abstract – We propose a circuit to directly connect a differential capacitive sensor to a microcontroller unit (MCU), which is based on the charge-transfer method and does not need any calibration component. The performance has been tested by emulating the differential capacitive sensor with discrete components. The major uncertainty sources are residual stray capacitances. The maximal deviation obtained, referred to the Full Scale Span (FSS), is ±4 % for sensors with nominal capacitance C_0 = 100 pF, and ±0,6 % for sensors with C_0 = 1 nF.

Keywords: Differential capacitive sensor, charge transfer, sensor-to-microcontroller interface, direct sensor interface

1. BASIC INFORMATION

Differential capacitive sensors are widely used to measure linear or angular position and displacement, pressure, force, and acceleration, as described, for example, in [1]–[4]. Their electrical model are two sensing capacitances (i.e. C_1 and C_2) with a movable common electrode (C), as shown in Fig 1, whose values change with respect to the physical quantity being sensed in equal proportion but in opposite directions.

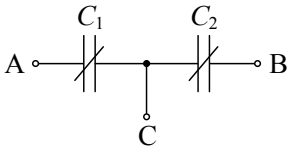

Fig. 1. Equivalent circuit of a differential capacitive sensor.

Depending on the effect of the movement of C, the change in the sensor's capacitances C_1 and C_2 has a linear or hyperbolic characteristic that can be expressed by [5],

$$C_1 = C_0(1+x),\ C_2 = C_0(1-x) \tag{1}$$

$$C_1 = \frac{C_0}{1-x},\ C_2 = \frac{C_0}{1+x} \tag{2}$$

where C_0 is the resting value of C_1 and C_2 and x is the relative change of capacitance, hence $-1 < x < +1$. In both cases, x can be calculated from

$$x = \frac{C_1 - C_2}{C_1 + C_2} \tag{3}$$

Signal interfaces for capacitive sensors are usually based on voltage divider circuits and derivatives thereof such as dc bridges and pseudo-bridges, or on sinusoidal or relaxation oscillators [6]–[9]. These circuits rely on either analogue components and analogue-to-digital converters (ADC) or time/frequency measurements [8], [9]. Usually, the resulting signal is acquired, stored, processed, displayed and/or communicated to other devices or systems via a digital unit (e.g., a MCU). This measurement chain is implemented in some commercial integrated circuits (ICs) that integrate, for example, the signal conditioning circuit, the ADC and/or MCU, such as AD7745 (Analog Devices), ZSSC3122 (ZMDI), MS3110 (Irvine Sensors), or the oscillator, such as UTI (Smartec). Overall, the number of components in discrete solutions or the use of specialized ICs with no second source supplier available hinders the design of cost-effective solutions based on these approaches.

Differential capacitive sensors can be measured by a MCU as single active component [4], [10]. The MCU measures the time interval needed to discharge the sensors to a given threshold voltage through a reference resistor R_r, without any intermediate electronics. Hence, these interface circuits are cost-effective solutions because only the sensor and a MCU are required. Nevertheless, to obtain the best speed–accuracy trade off when measuring capacitances on the order of 100 pF, they need $R_r > 20$ MΩ, which may increase electronic noise and external interference (EMI).

Here we propose a direct interface circuit based on the charge-transfer method, where the unknown capacitance is calculated by counting the number of charge-transfer cycles needed to charge a reference capacitor to a threshold voltage via the capacitive sensor. In contrast with [4] and [10], the circuit does not include any large resistor hence its susceptibility to noise and EMI should be lower. Furthermore, the MCU does not need to include even a timer. The charge-transfer-based method is used in switched capacitor circuits that implement resistances in ICs [11] and have good ability to reject external EMI. In a previous work [12], we analysed the susceptibility of these circuits for single capacitive sensors to uncertainty sources such as stray capacitance and temperature and power supply voltage drifts, and proposed design solutions to reduce their effect. This paper extends that analysis to differential capacitive sensors with values from 100 pF to 1 nF, considers the limitations when stray capacitances are accounted for, and proposes novel measurement methods to overcome them.

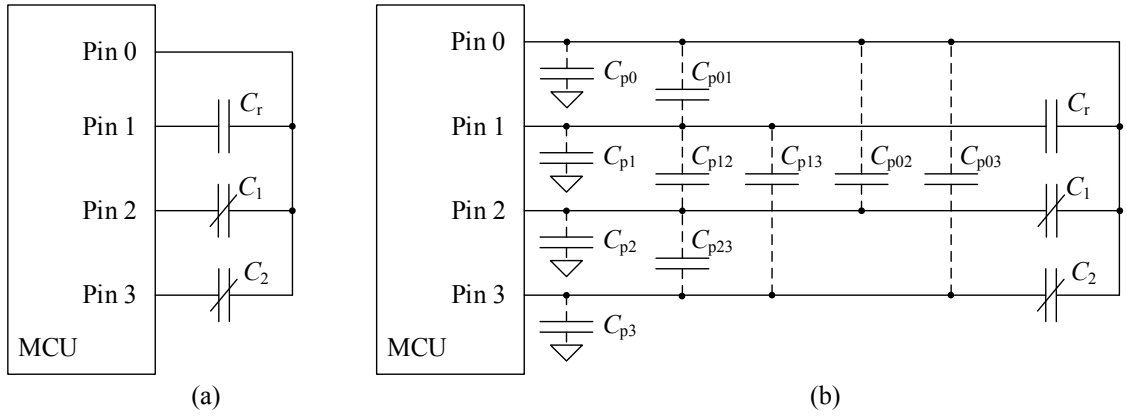

Fig. 2. Charge-transfer-based signal interface for a differential capacitive sensor: (a) Basic circuit; (b) Circuit when parasitic capacitances to ground and between pins from each MCU pins involved in the measurement are considered.

2. DESCRIPTION AND ANALYSIS OF THE INTERFACE CIRCUIT PROPOSED

2.1. Operating principle

Fig. 2(a) shows the charge-transfer-based circuit proposed to measure a differential capacitive sensor. C_1 and C_2 are two capacitances that model the sensor. C_r is a known reference capacitor, such that $C_r >> C_1 + C_2$. Pins #0 to #3 are digital input/output (I/O) pins that can be configured as any of three states: (a) LOW digital output ("0"), i.e. a voltage V_{OL} with equivalent internal resistance R_{OL}; (b) HIGH digital output ("1"), i.e. a voltage V_{OH} with equivalent internal resistance R_{OH}; and (c) high-impedance input (HZ).

The procedure is similar to that proposed in [12]–[14] to measure a single capacitive sensor. The measurement method involves three stages: 1) discharging (only at the beginning of each new measurement); 2) charging; and 3) charge-transfer and counting of the number of charge-transfer cycles. In the discharging stage, pins #0 to #3 are set as outputs that provide a "0", hence C_1, C_2, and C_r are discharged towards V_{OL} with a time constant $\tau_D \approx 2R_{OL}C_r$. In the charging stage, pin #0 is set as an output that provides an "1", whereas pin #1 is set as an input; therefore, C_1, C_2 or both will be charged toward V_{OH} if pins #2, #3 or both are set to "0" respectively. Finally, in the charge-transfer stage, pins #2 and #3 remain in their previous state, pin #1 is set as an output that provides a "0", pin #0 is set as an input, and the control program starts counting the number of charge transfer cycles. In this configuration, part of the charge stored in C_1, C_2 or both is transferred to C_r, and pin #0 acts as a voltage threshold detector. By repeating the charge transfer cycle (stages 2 and 3), C_r is exponentially charged toward V_{OH}. After a finite sequence of N charge transfer cycles, if the charging stage lasts long enough for C_1, C_2 or both to fully charge to V_{OH}, the voltage across C_r is

$$V_r[N] = \frac{C_{eq}}{C_{eq}+C_r}(V_{OH}-V_{OL}) + \frac{C_r}{C_x+C_r}V_r[N-1] \quad (4)$$

where C_{eq} is C_1, C_2, or $C_1 + C_2$. The first term on the right side results from the charge transferred during that cycle, and the second term results from the charge transferred during the previous $N-1$ cycles. If $V_{OL} \approx 0$ V, thanks to the initial discharging stage, and $C_r >> C_1 + C_2$, the number N_{eq} of charge transfer cycles needed to charge C_r to a given threshold voltage V_T, say $V_r[N_{eq}] = V_T$, is [12]

$$N_{eq} = \frac{C_r}{C_{eq}} \ln\left(\frac{V_{OH}}{V_{OH}-V_T}\right) = \frac{k}{C_{eq}} \quad (5)$$

where $k = C_r \ln[V_{OH}/(V_{OH} - V_T)]$. The circuit in Fig. 2 measures C_1, then C_2 and finally $C_1 + C_2$ to determine x from (3). Measuring $C_1 + C_2$ reduces the effects of some stray capacitances, as shown in the next section. Table 1 summarizes the state of pins #2 and #3 in Fig. 2(a) during the charging stage, the equivalent capacitance C_{eq}, and the number N_{eq} of charge-transfer cycles for each of the three measurements.

From (5) and the formulae in Table 1, if k remains constant during the whole process, we have

$$x^* = \frac{N_{C12}(N_{C2}-N_{C1})}{N_{C1}N_{C2}} \quad (6)$$

that is independent of k, hence from V_{OH}, V_T, and C_r. Each stage of the measurement process must last long enough to ensure that the final voltage across C_{eq} and C_r is close enough to its ideal value. By waiting for $T_D > 10\tau_D$ for the discharging stage, $T_C > 10(R_{OH} + R_{OL})(C_1 + C_2)$ for the charging stage, and $T_R > 20R_{OL}(C_1 + C_2)$ for charge-transfer stage, the relative deviation of the final voltage is less than 0.005 %. Furthermore, a long T_D reduces dielectric absorption effects in C_{eq} and C_r [15].

Table 1. State of pins #2 and #3 [Fig. 2(a)], equivalent capacitances C_{eq} and resulting charge transfer cycles for each of the three measurements, where $k = C_r \ln[V_{OH}/(V_{OH} - V_T)]$.

C_{eq} measured	Pin #2	Pin #3	N_{eq}
C_1	"0"	HZ	$N_{C1} = k/C_1$
C_2	HZ	"0"	$N_{C2} = k/C_2$
$C_1 + C_2$	"0"	"0"	$N_{C12} = k/(C_1 + C_2)$

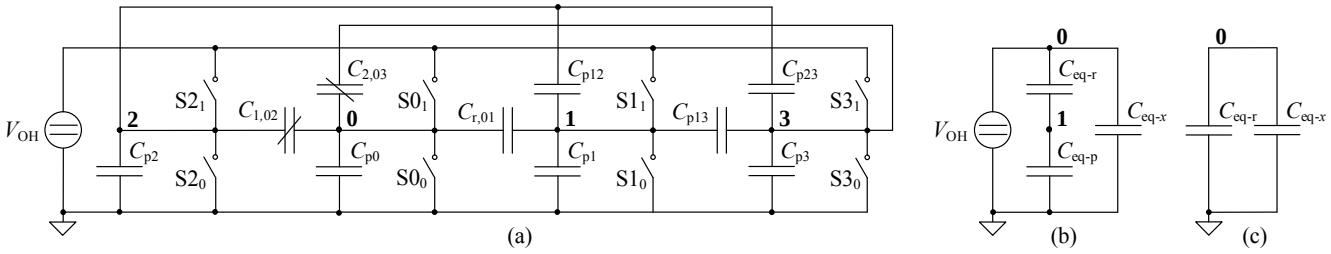

Fig. 3. Equivalent circuit for Fig. 2: (a) When logic states of each MCU pins involved in the measurement are modelled by using switches, and parasitic capacitances to ground and between pins are considered; (b) and (c) During the charging and charge-transfer stages, respectively. $C_{r,01} = C_r + C_{p01}$, $C_{1,02} = C_1 + C_{p02}$, and $C_{2,03} = C_2 + C_{p03}$.

2.2. Effect of Parasitic Capacitances

Equation (6) is simple and compact but disregards the parasitic capacitances to ground and between all MCU pins involved in the measurement, shown in Fig. 2(b) that mainly depend on the layout of the circuit to connect C_r, C_1 and C_2, the input impedance of each MCU pin and the distance between them, whose value is a few picofarads [16].

If $V_{OL} = 0$ V during the charge-transfer process, the interface circuit in Fig. 2(b) may be simplified to that in Fig. 3(a) with $C_{r,01} = C_r + C_{p01}$, $C_{1,02} = C_1 + C_{p02}$ and $C_{2,03} = C_2 + C_{p03}$. The setting of MCU pins as outputs that provide a "0" and "1" in Fig. 3(a) is respectively modelled by the closing of $S0_0$ and $S0_1$, $S1_0$ and $S1_1$, $S2_0$ and $S2_1$, and $S3_0$ and $S3_1$. Similarly, their setting as inputs is modelled by opening both switches. During the charging and charge-transfer stages, the equivalent capacitances in the interface circuit may be respectively simplified to those in Fig. 3(b) and Fig. 3(c). By applying the operating principle explained in Section 2.1, the number $N_{eq\text{-}s}$ of charge transfer cycles for the equivalent capacitance $C_{eq\text{-}x}$ from to pin #0 to ground is

$$N_{eq\text{-}s} = \frac{C_{eq\text{-}r}}{C_{eq\text{-}x}} \ln\left(\frac{V_{OH}}{V_{OH} - V_T}\right) = \frac{k}{C_{eq\text{-}x}} \tag{7}$$

where $C_{eq\text{-}r}$ and $C_{eq\text{-}p}$ are the respective equivalent capacitances between pin #0 and pin #1, and from pin #1 to ground. Table 2 summarizes the expressions for $C_{eq\text{-}x}$, $C_{eq\text{-}r}$ and $C_{eq\text{-}p}$ when measuring C_1, C_2 and $C_1 + C_2$.

In order to simplify the analysis, in Table 2 we assume $C_p \approx C_{p1} \approx C_{p0} \approx C_{p02} \approx C_{p03}$, which is probably true when the sensor and C_r are next to the MCU. Hence, replacing the respective $N_{eq\text{-}s}$ in (6) for each measurement, we have

$$x^* \approx \frac{C_1 - C_2}{C_1 + C_2 + 4C_p + C_{p12} + C_{p13}} \tag{8}$$

Therefore, several stray capacitances are compensated but some systematic deviation remains that will be more relevant for small capacitive sensors.

3. EXPERIMENTAL SETUP

The signal interface circuit proposed has been validated by implementing it with a PIC16F84A connected to a 4 MHz crystal oscillator, as shown in Fig. 4. The instruction cycle time was 1 µs. The PIC16F84A is a low-end MCU without any timer. The control program was written in assembler language. The function of pins #0, #1, #2 and #3 were respectively implemented by pins RB0, RB1, RB3 and RB7. C_1 and C_2 were ceramic capacitors from 1 pF to 1 nF with 10 % tolerance. C_r was 1,0 µF, with metalized polyester dielectric. First, C_1 was a single capacitor and C_2 was a high-value capacitor in parallel with several low-value capacitors so that $C_1 \approx C_2$. Then, the different values of x were obtained by moving, one by one, a low-value capacitor from C_2 to C_1 thus resulting in the same but opposite change in C_1 and C_2.

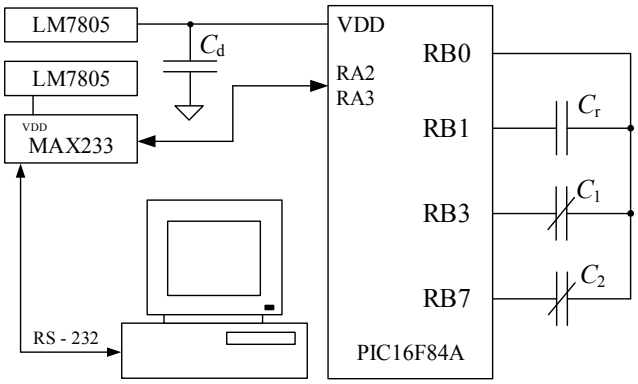

Fig. 4. Experimental setup designed to evaluate the charge-transfer-based signal interface for differential capacitive sensors.

C_1, C_2, and C_r were measured with an impedance analyser (Agilent 4294A) connected to a test fixture (Agilent 16047E), which basic relative uncertainty is better than ±1 % from 1 pF to 1 nF, when measuring at 100 kHz and 0,5 V (rms oscillator output level). T_D, T_C, and T_R were calculated from the minimal R_{OL} and maximal R_{OH} values for pins RB0, RB1, RB3, and RB7, indirectly measured by the voltage-divider technique described in [7].

Each capacitor was measured 100 times, hence obtaining 100 values for N_x, N_{c1}, and N_{c2}. These values were sent to a personal computer via a serial link (EIA-232) implemented with a MAX233 IC and the RA2 and RA3 MCU pins, under LabVIEW control. Next, we calculated 100 values of x^* from (6), their mean x^*_{av}, and its deviation relative to the Full Scale Span (FSS), RD = $(x - x^*_{av})$/FSS.

Measurement uncertainty was reduced by applying design solutions proposed in [7] and [12]. External interference was reduced by configuring unused MCU I/O pins as inputs and connecting them to ground. Parasitic capacitance to ground was reduced by excluding any ground plane in the PCB. Power supply noise effects were reduced by supplying the MCU and MAX233 by a separate voltage regulator each (LM7805), and by connecting a decoupling capacitor $C_d = 100$ nF between the MCU power supply pin and ground.

Table 2. Equivalent capacitances between pin #0 and pin #1 ($C_{eq\text{-}r}$), and to ground ($C_{eq\text{-}x}$ and $C_{eq\text{-}p}$), when measuring N_{C1}, N_{C2}, and N_{C12}.

C_{eq} measured	$C_{eq\text{-}x}$	$C_{eq\text{-}r}$	$C_{eq\text{-}p}$
C_1	$C_1 + C_{p0} + C_{p02} + \dfrac{(C_2 + C_{p03})(C_{p3} + C_{p23})}{C_2 + C_{p03} + C_{p13} + C_{p23} + C_{p3}}$	$C_r + C_{p01} + \dfrac{C_{p13}(C_2 + C_{p03})}{C_{p03} + C_{p13} + C_{p23} + C_{p3} + C_2}$	$C_{p1} + C_{p12} + \dfrac{C_{p13}(C_{p3} + C_{p23})}{C_2 + C_{p03} + C_{p13} + C_{p23} + C_{p3}}$
C_2	$C_2 + C_{p0} + C_{p03} + \dfrac{(C_1 + C_{p02})(C_{p2} + C_{p23})}{C_1 + C_{p02} + C_{p12} + C_{p2} + C_{p23}}$	$C_r + C_{p01} + \dfrac{C_{p12}(C_1 + C_{p02})}{C_{p02} + C_{p12} + C_{p2} + C_{p23} + C_1}$	$C_{p1} + C_{p13} + \dfrac{C_{p12}(C_{p2} + C_{p23})}{C_{p02} + C_{p12} + C_{p2} + C_{p23} + C_1}$
$C_1 + C_2$	$C_1 + C_2 + C_{p0} + C_{p02} + C_{p03}$	$C_r + C_{p01}$	$C_{p1} + C_{p12} + C_{p13}$

4. EXPERIMENTAL RESULTS AND DISCUSSION

R_{OL} and R_{OH}, for pins RB0, RB1, RB3 and RB7 were below 50 Ω and 125 Ω, respectively, $C_{eq\text{-}max}$ was 1,95 nF and C_r 1,01 µF. Consequently, T_D, T_C and T_R should respectively be larger than 1,01 ms, 2,9 µs and 2,9 µs. T_D was selected 10 ms to reduce dielectric absorption in C_r [15]. T_C and T_R were respectively selected 5 µs and 25 µs by considering the minimal number of instructions to execute at each stage of the charge-transfer measurement process.

Fig. 5 shows x^*_{av} calculated from 100 values of x^* obtained by (6), versus the applied x calculated by (3), for the two ranges measured. The maximal RD was ±0,04 FSS for $C_0 = 100$ pF, Fig. 5(a), and ±0,006 FSS for $C_0 = 1$ nF, Fig. 5(b). According to (8), parasitic capacitances, which for a previous similar setup we estimated to be about 10 pF [12], yield large measurement deviations. The gain effect observed can be attributed to internal charge injection into the output stage of MCU pins [17]. Nevertheless, these relative deviations can be acceptable in cost-constrained industrial applications.

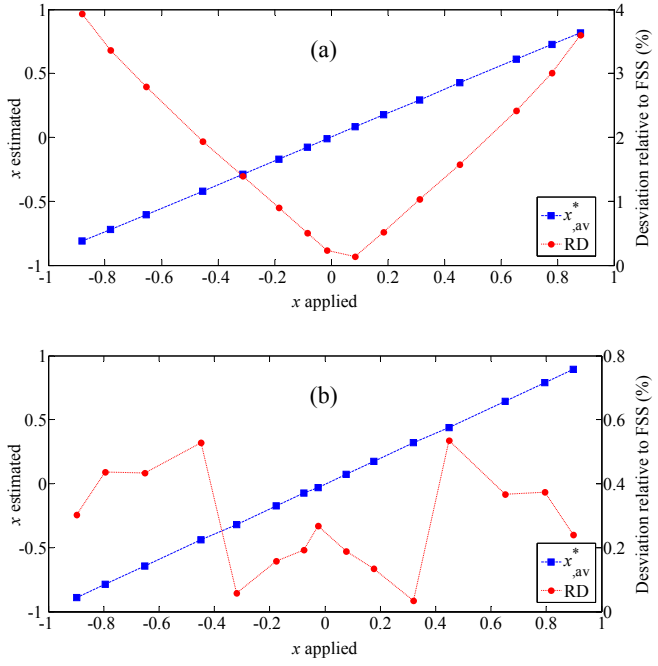

Fig. 5. Relative deviation for the circuit in Fig. 2 when measuring a differential capacitive sensor with (a) $C_0 = 100$ pF and (b) 1 nF.

5. CONCLUSIONS

A novel charge-transfer-based circuit to measure differential capacitive sensors has been proposed that can be implemented by low-end MCUs without any timer. The method comprises the separate measurement of each capacitance and of both capacitances connected in parallel. This makes the result independent from MCU parameters (V_{OH} and V_T) and obviates the need of calibration components, large resistors, or electric shielding. Further, several parasitic capacitances to ground and between MCU pins have no effect and the effect of the remaining ones is a maximal relative deviation of ±0,04 FSS for 100 pF sensors and ±0,006 FSS for 1 nF sensors.

ACKNOWLEDGMENTS

Jorge E. Gaitán-Pitre was supported by a joint-grant from BarcelonaTech (UPC) and SEAT Technical Centre. The authors would like to thank the Castelldefels School of Telecommunications and Aerospace Engineering for its research facilities and Mr. F. López for his technical support.

REFERENCES

[1] C. R. Merritt, H. T. Nagle, and E. Grant, "Textile-based capacitive sensors for respiration monitoring," *IEEE Sens. J.*, vol. 9, no. 1, pp. 71–78, January 2009.

[2] B. George and V. J. Kumar, "Analysis of the switched-capacitor dual-slope capacitance-to-digital converter," *IEEE Trans. Instrum. Meas.*, vol. 59, no. 5, pp. 997–1006, May 2010.

[3] M. I. Tiwana, A. Shashank, S. J. Redmond, and N. H. Lovell, "Characterization of a capacitive tactile shear sensor for application in robotic and upper limb prostheses," *Sensors Actuators A Phys.*, vol. 165, no. 2, pp. 164–172, February 2011.

[4] F. Reverter and Ò. Casas, "Interfacing differential capacitive sensors to microcontrollers: a direct approach," *IEEE Trans. Instrum. Meas.*, vol. 59, no. 10, pp. 2763–2769, October 2010.

[5] K. Mochizuki, T. Masuda, and K. Watanabe, "An interface circuit for high-accuracy signal processing of differential-capacitance transducers," *IEEE Trans. Instrum. Meas.*, vol. 47, no. 4, pp. 823–827, August 1998.

[6] R. Pallàs-Areny and J. G. Webster, *Sensors and Signal Conditioning*, 2nd ed., John Wiley & Sons, New York, 2001.

[7] F. Reverter and R. Pallàs-Areny, *Direct Sensor-to-Microcontroller Interface Circuits: Design and Characterisation*, Marcombo, Barcelona, 2005.

[8] N. M. Mohan, B. George, and V. J. Kumar, "A novel dual-slope resistance-to-digital converter," *IEEE Trans. Instrum. Meas.*, vol. 59, no. 5, pp. 1013–1018, May 2010.

[9] J. H.-L. Lu, M. Inerowicz, S. Joo, J.-K. Kwon, and B. Jung, "A low-power, wide-dynamic-range semi-digital universal sensor readout circuit using pulsewidth modulation," *IEEE Sens. J.*, vol. 11, no. 5, pp. 1134–1144, May 2011.

[10] F. Reverter and Ò. Casas, "Direct interface circuit for differential capacitive sensors," in *IEEE Instrumentation and Measurement Technology Conference - I2MTC*, pp. 1609–1612, Victoria, BC, Canada, 2008.

[11] P. E. Allen and E. Sánchez-Sinencio, *Switched Capacitor Circuits*, Van Nostrand Reinhold, New York, 1984.

[12] J. E. Gaitán-Pitre, M. Gasulla, and R. Pallàs-Areny, "Analysis of a direct interface circuit for capacitive sensors," *IEEE Trans. Instrum. Meas.*, vol. 58, no. 9, pp. 2931–2937, September 2009.

[13] H. Philipp, "Charge transfer capacitance measurement circuit," US6466036B1, 15-Oct-2002.

[14] P. H. Dietz, D. Leigh, and W. S. Yerazunis, "Wireless liquid level sensing for restaurant applications," in *Proceedings of IEEE Sensors*, pp. 715–720, vol. 1, Orlando, Florida, Jun. 2002.

[15] J. C. Kuenen and G. C. M. Meijer, "Measurement of dielectric absorption of capacitors and analysis of its effects on VCO's," *IEEE Trans. Instrum. Meas.*, vol. 45, no. 1, pp. 89–97, February 1996.

[16] H. W. Johnson, *High-Speed Digital Design: A Handbook of Black Magic*, 2nd ed., Prentice Hall, 1993.

[17] Y. Villavicencio, F. Musolino, and F. Fiori, "Electrical model of microcontrollers for the prediction of electromagnetic emissions," *IEEE Trans. Very Large Scale Integr. Syst.*, vol. 19, no. 7, pp. 1205–1217, July 2011.